

REPORT DOCUMENTATION PAGE		Form Approved OMB NO. 0704-0188	
Public Reporting Burden for this collection of information is estimated to average 1 hour per response, including the time for reviewing instructions, searching existing data sources, gathering and maintaining the data needed, and completing and reviewing the collection of information. Send comment regarding this burden estimate or any other aspect of this collection of information, including suggestions for reducing this burden, to Washington Headquarters Services, Directorate for Information Operations and Reports, 1215 Jefferson Davis Highway, Suite 1204, Arlington VA, 22202-4302, and to the Office of Management and Budget, Paperwork Reduction Project (0704-0188), Washington DC 20503			
1. AGENCY USE ONLY (Leave Blank)		2. REPORT DATE: 20-Jul-2007	3. REPORT TYPE AND DATES COVERED Final Report 25-Apr-2004 - 24-Apr-2007
4. TITLE AND SUBTITLE High Performance Damping with Carbon Nanotube-Polymer Composites			5. FUNDING NUMBERS W911NF-04-1-0111
6. AUTHORS Kon-Well Wang, Charles Bakis			8. PERFORMING ORGANIZATION REPORT NUMBER
7. PERFORMING ORGANIZATION NAMES AND ADDRESSES Pennsylvania State University Office of Sponsored Programs The Pennsylvania State University University Park, PA 16802 -			
9. SPONSORING/MONITORING AGENCY NAME(S) AND ADDRESS(ES) U.S. Army Research Office P.O. Box 12211 Research Triangle Park, NC 27709-2211			10. SPONSORING / MONITORING AGENCY REPORT NUMBER 45565-EG.3
11. SUPPLEMENTARY NOTES The views, opinions and/or findings contained in this report are those of the author(s) and should not contrued as an official Department of the Army position, policy or decision, unless so designated by other documentation.			
12. DISTRIBUTION AVAILABILITY STATEMENT Distribution authorized to U.S. Government Agencies Only, Contains Proprieta		12b. DISTRIBUTION CODE	
13. ABSTRACT (Maximum 200 words) The abstract is below since many authors do not follow the 200 word limit			
14. SUBJECT TERMS Structural Damping, Carbon Nanotubes, Composites			15. NUMBER OF PAGES Unknown due to possible attachments
			16. PRICE CODE
17. SECURITY CLASSIFICATION OF REPORT UNCLASSIFIED	18. SECURITY CLASSIFICATION ON THIS PAGE UNCLASSIFIED	19. SECURITY CLASSIFICATION OF ABSTRACT UNCLASSIFIED	20. LIMITATION OF ABSTRACT UL

Report Title

High Performance Damping with Carbon Nanotube-Polymer Composites

ABSTRACT

The overall goal of this research project is to investigate the characteristics of carbon nanotube (CNT) filler -based polymers and provide guidelines to advance the state of the art of structural damping enhancement utilizing CNT fillers. Our major efforts have been focused on: (a) To perform tests to observe the damping effect of composites with CNT fillers; (b) To develop a micromechanical constitutive model to analyze the effects of the “stick-slip” motion of the filler-filler and filler-resin interactions on the total loss factor of composite with aligned and randomly oriented, dilute nanoropes; (c) To simultaneously analyze the effects of the viscoelastic resin together with the “stick-slip” motion of the filler-filler and filler-resin interactions on the total loss factor of composite with dilute nanoropes; (d) To utilize molecular dynamics (MD) simulations to analyze the interfacial strength at the filler-filler and filler-resin interface; and (e) To develop methods for nanofiller alignment in composites.

List of papers submitted or published that acknowledge ARO support during this reporting period. List the papers, including journal references, in the following categories:

(a) Papers published in peer-reviewed journals (N/A for none)

X. Zhou, E. Shin, K. W. Wang, and C. E. Bakis, “Interfacial Damping Characteristics of Carbon Nanotube-Based Composites,” *Composites Science and Technology*, 64(15), pp. 2425-2437, 2004.

A. Liu, J. H. Huang, K. W. Wang, C. E. Bakis, “Effects of Interfacial Friction on the Damping Characteristics of Composites Containing Randomly Oriented Carbon Nanotube Ropes,” *Journal of Intelligent Material Systems and Structures*, 17, pp. 217-229, 2006.

Number of Papers published in peer-reviewed journals: 2.00

(b) Papers published in non-peer-reviewed journals or in conference proceedings (N/A for none)

Number of Papers published in non peer-reviewed journals: 1.00

(c) Presentations

Number of Presentations: 0.00

Non Peer-Reviewed Conference Proceeding publications (other than abstracts):

Ailin Liu, K. W. Wang, Charles E. Bakis, Jin H. Huang, “Analysis of Damping Characteristics of a Viscoelastic Polymer Filled with Randomly Oriented Single-Wall Nanotube Ropes,” *SPIE Conf. on Smart Structures and Materials*, San Diego, CA, 2006.

Number of Non Peer-Reviewed Conference Proceeding publications (other than abstracts): 1

Peer-Reviewed Conference Proceeding publications (other than abstracts):

Number of Peer-Reviewed Conference Proceeding publications (other than abstracts): 0

(d) Manuscripts

Number of Manuscripts: 0.00

Number of Inventions:

Graduate Students

<u>NAME</u>	<u>PERCENT SUPPORTED</u>
Ailin Liu	0.50
Ambuj Sharma	0.15
FTE Equivalent:	0.65
Total Number:	2

Names of Post Doctorates

<u>NAME</u>	<u>PERCENT SUPPORTED</u>
Xu Zhou	0.05
Jin Huang	0.05
FTE Equivalent:	0.10
Total Number:	2

Names of Faculty Supported

<u>NAME</u>	<u>PERCENT SUPPORTED</u>	National Academy Member
Charles Bakis	0.05	No
Kon-Well Wang	0.05	No
FTE Equivalent:	0.10	
Total Number:	2	

Names of Under Graduate students supported

<u>NAME</u>	<u>PERCENT SUPPORTED</u>
FTE Equivalent:	
Total Number:	

Student Metrics

This section only applies to graduating undergraduates supported by this agreement in this reporting period

The number of undergraduates funded by this agreement who graduated during this period:	0.00
The number of undergraduates funded by this agreement who graduated during this period with a degree in science, mathematics, engineering, or technology fields:.....	0.00
The number of undergraduates funded by your agreement who graduated during this period and will continue to pursue a graduate or Ph.D. degree in science, mathematics, engineering, or technology fields:.....	0.00
Number of graduating undergraduates who achieved a 3.5 GPA to 4.0 (4.0 max scale):	0.00
Number of graduating undergraduates funded by a DoD funded Center of Excellence grant for Education, Research and Engineering:	0.00
The number of undergraduates funded by your agreement who graduated during this period and intend to work for the Department of Defense	0.00
The number of undergraduates funded by your agreement who graduated during this period and will receive scholarships or fellowships for further studies in science, mathematics, engineering or technology fields:	0.00

Names of Personnel receiving masters degrees

<u>NAME</u>
Total Number:

Names of personnel receiving PhDs

<u>NAME</u>

Total Number:

Names of other research staff

<u>NAME</u>

<u>PERCENT SUPPORTED</u>

FTE Equivalent:

Total Number:

Sub Contractors (DD882)

Inventions (DD882)

High Performance Damping with Carbon Nanotube-Polymer Composites

Proposal No. 45565-EG

**K. W. Wang and Charles Bakis
The Pennsylvania State University
University Park, PA 16802**

TABLE OF CONTENTS

	Page Number
Table of Contents	1
List of Illustrations	2
Statement of the Problem Studied	4
Summary of the Most Important Results	4
List of Publications	
Referred Journal Publication	13
Conference Publications and Presentations	14
Participants	14

LIST OF ILLUSTRATIONS

	Page Number
Figure 1. Ultrasonic mixer set-up used for dispersing nanotubes in resin mixture	15
Figure 2. Loss factor measurements through dynamic testing	15
Figure 3. Loss factor vs. peak cyclic strain: neat resin and 1 wt% CNT specimens	15
Figure 4. A schematic of a nanotube lattice in hexagonal arrangement	16
Figure 5. A schematic of load transfer in the tube lattice model	16
Figure 6. Loss factors: nanoropes vs nanotubes	16
Figure 7. Unit cell consisting of a bundle of seven SWNTs surrounded by a sheath and remote resin	17
Figure 8. Comparison of composites containing randomly dispersed and oriented nanoropes	17
Figure 9. Comparison for composites containing aligned SWNTs and aligned nanoropes	18
Figure 10. Comparison for composites containing aligned nanoropes and randomly dispersed nanoropes	18
Figure 11. Composites using standard solid model	19
Figure 12. Loss factors vs. magnitude of applied stress	19
Figure 13. Interfacial shear strength between nanotube ropes as a function of tube length	20
Figure 14. Interfacial shear strength between nanotube and epoxy as a function of tube length	20
Figure 15 Electrical measurements on aligned and random nanofiber composites	21
Figure 16. Effect of DC electric field on the alignment of CNFs in epoxy	21
Figure 17. Kinetics of CNF alignment in AC electric field	22
Figure 18. Chain of aligned CNFs in the direction of AC electric field	23

Figure 19. Chains of CNFs in epoxy bridging the gap between the electrodes at various AC frequencies ($V_{\text{rms}} = 50 \text{ V}$; distance between electrodes = 1 mm)	23
Figure 20. Chains of 0.1 wt% aligned CNFs in a fully cured epoxy	24
Figure 21. Fully cured 0.1 wt% aligned CNF/epoxy composite	24

STATEMENT OF THE PROBLEM STUDIED

The unique features that make carbon nanotubes (CNTs) ideal fillers for high performance damping composites are their *large surface area*, *large aspect ratio*, *high stiffness*, *low density*, and *high thermal conductivity* characteristics. Because of their nanometer scale radius and low density, the surface area to mass ratio of carbon nanotubes is extremely large. Given the high aspect ratio, high stiffness, and large surface area of CNTs, it is anticipated that tremendous energy dissipation and structural damping can be achieved by taking advantage of the interfacial stick-slip friction between CNTs and polymer resins and between bundled CNTs. In addition, due to low density and high thermal conductivity (heat dissipation ability) of the CNT composites, such a high performance damping material could be light and compact. Despite their wonderful potential, the damping characteristics of such composites have not been explored in any detail.

In a previous ARO-supported STIR project, the Penn State researchers (Wang and Bakis) have made good progress in developing a structural damping model of CNT-based composites by assuming stick-slip interfacial friction between CNT and resin. The developed model concludes that such stick-slip mechanism leads to a strain-dependent damping enhancement. The trend of the analytical findings was qualitatively observed in experimental results. However, in this previous study, the loss factors were experimentally characterized using free vibration testing of beams in flexure, implying that the material is not in a uniform, steady state of strain. In addition, only completely dispersed individual single-walled nanotubes (SWNTs) were modeled, implying that the effects of nanotube aggregates and inter-tube interactions were ignored; while in reality, the CNTs usually exist in the state of bundles in polymers and formed the so-called nanotube ropes or nanoropes. Finally, the effects of various system parameters (such as filler orientations, interfacial strength) were not explicitly explored.

The overall goal of the research presented in this report is to advance the state of the art of structural damping by utilizing the characteristics of carbon nanotube-based polymers, building upon the previous Penn State experience in active/passive damping and CNT-based composite materials.

SUMMARY OF THE MOST IMPORTANT RESULTS

Experimental observations

An experimental investigation using direct uniaxial testing has been conducted to investigate the energy dissipation characteristics of polymeric composites containing carbon nanotube fillers. In this case, we can obtain results with a steady, uniform strain field in the specimens. The specimens were fabricated by directly mixing single-walled carbon nanotubes into representative polymers, such as epoxy, with high-power ultrasonic agitation (Figure 1). To characterize loss factors, uniaxial testing with harmonic loading was conducted to directly measure the phase lag between stress and strain (Figure 2). The loss factors were measured over a range of applied strain amplitudes. Experimental investigations were performed on the neat resin and specimens with CNT fillers. The comparison of loss factors as a function of applied strain amplitude is shown in Figure 3. It can be observed that the neat resin exhibits a slight and relatively smooth

variation in loss factor in the entire tested strain range. The measured loss factor of the neat resin is around 1%, which is a typical value for epoxy. However, the energy dissipating characteristics of the specimen with CNTs (in this example, 1 wt%) are significantly different from that of the specimen without CNTs. Figure 3 shows that energy loss can be enhanced by adding CNTs. For the material containing CNTs, the loss factor first increases with increasing strain to a certain value (around 100 $\mu\epsilon$, in this case), and then decreases for further increases in strain. A clear peak of 5% in loss factor is found for the specimen with CNTs. These phenomena support the existence of a stick-slip motion between the resin and nanotubes.

Nanorope-based composites modeling and analysis -- damping due to filler interfacial actions

A constitutive model including both principal elastic modulus and loss factor was developed for carbon nanorope-based polymeric composites. In contrast to the model developed in the aforementioned Penn State STIR program (with the assumption of completely dispersed SWNTs), the characteristics of nanoropes and inter-tube effects are considered in this new model. Bundled CNTs were modeled using a close-packed lattice consisting of seven SWNTs in a hexagonal array (Figure 4). The composite was described using a multi-phase system, composed of a resin, bonded and debonded nanotube ropes. The concept of stick-slip motion caused by frictional contacts was proposed to describe the load transfer behavior between the nanotubes and between the nanoropes and resin (Figure 5). A micromechanical model was developed to describe inter-tube and tube/resin frictional motions. Modulus change and energy dissipation due to the stick-slip interfacial load transfer were determined. The developed method was used to analyze composites with aligned nanoropes. Also, it was used to show the inter-tube sliding effects due to nanotube aggregation, where the elastic moduli and loss factors of composites filled with either well-dispersed nanotubes or nanoropes were compared to each other. Figure 6 shows the comparison of loss factors between these two composites with 1 vol. % nanotube fillers. Here, the critical interfacial shear stresses (bonding strength) were assumed to be 0.5 MPa for inter-tube interaction and 50 MPa for CNT-resin interaction. It can be seen that, for the well-dispersed nanotube composite, only one peak exists in the loss factor-strain curve, while the nanorope case has two. In the nanorope composite, the smaller peak in loss factor at a strain amplitude of about 500 $\mu\epsilon$ corresponds to slippage of the low strength interface between neighboring nanotubes within each nanorope, and the larger peak is mainly corresponding to the interaction between the CNTs and the resin. On the other hand, for the well-dispersed SWNT case, each SWNT in the composite is in full contact with the resin, and no inter-tube motion can occur; thus only one peak is generated in the loss factor-strain curve. As shown in the figure, in terms of overall damping, the maximum loss factor associated with well-dispersed nanotubes is higher than that with nanoropes. The reason is that the aggregation of the SWNTs in the form of ropes reduces the total contact surface between nanotubes and resin, thereby reducing the energy loss.

While the model of aligned nanoropes is novel and interesting, it is very restricted in applicability. Therefore, the model was further generalized for predicting the Young's modulus and damping of unaligned CNT nanorope reinforced polymers. A composite element consisting of a bundle of multiple SWNTs surrounded by a sheath of resin (Figure 7) is developed based on the off-axis short-fiber composite theories. The sheath carries all the shear stress between

carbon nanotubes and resin while the remote material is assumed to exhibit average composite properties. The concept of “stick-slip” motion caused by frictional contacts was proposed to describe the load transfer behavior between the nanotubes and between the nanotube ropes and the sheath. Due to the high aspect ratio of SWNTs and ropes, the load transfer at their ends was neglected. This approach was used to analyze composites containing well dispersed, randomly oriented CNT ropes and subject to quasi-static, monotonically increasing normal stress in one direction. The findings also illustrate the effects of inter-tube and tube/sheath sliding on damping and Young’s modulus in cases where the nanoropes are either uniaxially aligned or randomly oriented.

All the material properties used in the analysis are listed in Table 1. Based on previous investigations of bonding at inter-tube surfaces and SWNT/resin surfaces [Frankland et al, 2003; Wong et al., 2003; Cooper et al., 2002], the critical shear stress between nanotubes is around 0.5 MPa while that between multi-wall nanotubes (MWNTs) and resin ranges from 35 MPa to 500 MPa. Therefore, to show the effects of inter-tube and SWNT/resin interactions, three cases with different values of critical inter-tube and SWNT/resin shear stresses were used (Table 2).

The predicted relative Young’s moduli and loss factors are plotted in Figure 8. Here, the relative Young’s modulus is defined as the ratio of the Young’s modulus of the composite to that of the resin. While the relative Young’s modulus and the loss factors are plotted from the low to high stress range to illustrate the trend, the highest stresses shown in the figure might be difficult to achieve in realistic applications without breaking the specimen. Nevertheless, since these are only specific case studies and the stress level may change for different combinations of material properties, and the purpose of this investigation is to understand the general trend of the composite characteristics, it is important that we still discuss the entire stress range. The Young’s modulus first decreases slightly with stress as debonding occurs between nanotubes. Once the stress threshold for debonding at the SWNT/sheath interface is exceeded, the Young’s modulus decreases at an increasing rate with higher stress. As shown in Figure 8(b) and Figure 8(c), the loss factors are also stress-sensitive. In general, there are three distinct ranges in the loss factor-stress curve: the first one refers to the inter-tube debonding; the second one refers to the SWNT/sheath debonding; and the third one is due to the energy dissipation in post-debonding stage. In the small stress region (Figure 8(c)), the loss factors of Case 1 and Case 3 increase first (inter-tube debonding range) and then decrease slightly before further increasing (SWNT/sheath debonding range). Since Case 1 and Case 3 have the same inter-tube critical shear stresses, their first local peaks occur at the same stress value. In Case 1, the valley after the first peak is shallow because the SWNT/sheath slip occurs shortly after the inter-tube slip is fully developed. In Case 2, since the values of two critical shear stresses are closer than those of Cases 1 and 3, the SWNT/sheath sliding starts before the inter-tube sliding is fully developed at some off axial angles. Therefore, there is no decrease in loss factor between the onsets of the SWNT/sheath debonding and the inter-tube debonding. The effects of the two distinct slipping mechanisms merge together and form a continuous increase in the loss factor.

Figure 9 shows the Young’s moduli and loss factors of composites containing aligned individual SWNTs and composites with aligned nanoropes. The volume fractions of SWNTs in two cases are both 0.2%. The inter-tube and SWNT/sheath critical shear stresses are 0.5 MPa and 50 MPa, respectively; and the other properties of the resin and SWNTs are as listed in Table 1. For

composites with well-dispersed and aligned individual SWNTs, there is only one significant decrease in Young's modulus and two ranges of increase in loss factor because only SWNT/sheath friction exists. The maximum loss factor (within the applied stress range) of composites with aligned nanoropes (at stress value of 500 MPa), is about 10% less than that of aligned SWNTs (at stress value of 800 MPa), due to the decreased surface area at the nanotube/sheath interface. Also, for nanorope-based composites, the weaker inter-tube sliding hastens the onset of modulus decrease and damping increase in relation to the corresponding values for aligned SWNT composites.

Figure 10 shows the comparison of Young's modulus and loss factor for composites containing 0.2 vol% aligned nanoropes and randomly oriented nanoropes. The randomly oriented nanorope composite has a lower Young's modulus than the unidirectional nanorope reinforced composite over the entire stress range. For instance, at the stress level of 100 MPa, the Young's modulus of composites with randomly oriented nanoropes is only 80% of that with aligned nanoropes. Compared with the composites with aligned nanoropes, the loss factor of randomly oriented nanorope composites is higher when the stress level is the 100-350 MPa range. This is due to the fact that the sliding between the outer SWNTs and the sheath (also the inter-tube sliding) in composites with randomly oriented nanoropes occurs in lower stress regions than that of composites with aligned nanoropes. However, when the stress level exceeds 350 MPa, the loss factor of the aligned nanorope composites increases very quickly and reaches its maximum at 500 MPa, which is about 60% higher than the maximum value of composites with randomly oriented nanoropes (at 270 MPa). Again, the values of these applied stresses are acknowledged to be very high in comparison to the expected strength of these materials, but we are more interested in general trends and mechanisms in the current investigation.

From the analysis results, we arrive at the following conclusions:

- (a) For the cases studied, the composites with well aligned SWNTs have larger Young's modulus in all stress regions, as compared to composites with aligned or randomly oriented nanoropes. The inter-tube sliding weakens the load-capability of nanoropes and forces the onset of the SWNT/sheath sliding earlier. Due to the fact that the aspect ratio of nanotube is very large (about 1500) and the "stick-slip" interfacial movement is only considered to be significant along the length direction of nanoropes, the Young's modulus of composites containing randomly oriented nanoropes is even lower than those containing aligned nanoropes. This indicates that significant improvement of Young's modulus may be realized if one can fabricate CNT-based composites with fully-dispersed and well-aligned nanotubes.
- (b) For loss factor comparisons between cases with aligned SWNTs, aligned nanoropes, and randomly-oriented nanoropes, the conclusion could vary with different levels of applied stress. However, if the applied stress is high enough to cause complete sliding of all the SWNTs or nanorope fillers, and the maximum loss factors are compared for these cases, composites with fully-dispersed and well-aligned SWNTs will provide the highest loss factor and energy dissipation capability.

Nanorope-based composite modeling and analysis -- Combined damping effects of nanorope fillers and viscoelastic resins

While the studies presented in the previous section are necessary toward modeling the damping characteristics of nanorope-filled-composites, they are still limited by only focusing on the damping due to interfacial friction between adjacent nanotubes and between nanotubes and polymeric materials under monotonically increasing uniaxial loading. Since polymeric matrix materials possess viscoelastic properties, their rate-dependent characteristics need to be included in the CNT/polymer composite model and analyzed. To address such issues, a micromechanical constitutive model is proposed to simultaneously analyze the effects of viscoelastic resin and the “stick-slip” motion on the total loss factor of composite with randomly oriented, dilute nanoropes.

In the micromechanical model, the CNT-based composite is represented by a three-phase system composed of a resin, a resin sheath, and SWNT ropes as shown in Figure 7. The resin is described as a viscoelastic material using the three-element standard solid model. A Coulomb friction element represents nonlinear response due to the “stick-slip” movement at the SWNT/sheath and inner/outer SWNT interfaces. Since the aspect ratio of the nanotube is very large and the ‘stick-slip’ motion is only considered in the longitudinal direction of the nanotubes, the CNT-based composite is modeled as a viscoelastic element and a Coulomb friction element in parallel (Figure 11).

Figure 12 shows the loss factors of the composites with aligned nanoropes and randomly oriented nanoropes under uniaxial harmonic loading. For composites containing aligned nanoropes, the harmonic loading is applied in two directions: along the nanorope direction ($\theta=0^\circ$) and perpendicular to the nanorope direction ($\theta=90^\circ$). Three lines are plotted in each plot, referring to the total loss factor, loss factor due to viscoelastic resin, and loss factor caused by interfacial friction. Considering all the results in Figure 12, it is seen that the total effective loss factor is sensitive to the magnitude of the applied stress, while the loss factor of the viscoelastic resin is stress independent. In general, the three distinct ranges in the curve of loss factor due to the “stick-slip” motion are consistent with the analysis in previous section: the first one is between the start and completion of inter-tube debonding; the second one is caused by the start of SWNT/sheath debonding; and the third one is due to continuous sliding after all the nanotubes are fully debonded.

The composite with aligned nanoropes under loading along the nanorope direction (Figure 12(a)) shows the highest loss factor over the entire stress range. The energy dissipation contribution from “stick-slip” motion and viscoelastic material varies with alignment angle and applied stress level. For composites containing axially aligned nanoropes with 0° loading and randomly oriented nanoropes, the “stick-slip” friction is the main contribution for the total loss factor of the CNT-based composites even with small amount of nanotubes/ropes. However, for aligned nanoropes, after the off-axis angle is larger than some critical angle, the nanoropes undergo compression with tensile applied stress. In such cases, the importance of the loss factor due to viscoelastic material deformation increases and it even dominates the total loss factor when the magnitude of the applied stress is small. In general, the “stick-slip” motion dominates the total loss factor contribution at high stress levels.

Nanorope-based composite modeling and analysis -- Molecular dynamics simulation for interfacial shear strength prediction

Based on the micromechanical analysis in previous section, we realized that the “interfacial shear strength” is extremely important for predicting damping. One method to estimate such a parameter is to use molecular dynamics (MD) simulation. Both interfacial shear strengths between nanotube ropes and between nanotube and resins are calculated using a public domain software named DL_POLY.

In molecular dynamics simulation, the nanorope is modeled as seven nanotubes in a hexagonal array. The covalent bonding within the nanotubes is represented by the Tersoff potential. The non-bonding interactions between nanotubes are described by the Lennard-Jones potential. After equilibration of the system, the outer six nanotubes are fixed and a monotonically increasing normal force is applied to each atom of the inner nanotube in the tube length direction. The momentum balance model developed by Frankland [2003] is used to study the interface interaction. By monitoring the average velocity of the inner tube, we can obtain the threshold force to pull-out the inner tube. Therefore, the interfacial strength is simply the threshold force divided by the surface area of the inner tube.

The same concept is applied to calculate the interfacial shear strength between nanotube and epoxy resin. In this case, the epoxy resin is modeled using the OPLS force field including bond stretch, bond angle, torsion, and out-of-plane deformation. The Van der Waals energy between the nanotube and the epoxy is represented by Lennard-Jones potential.

Figure 13 shows the interfacial shear strength between the center and outer nanotubes in a rope as a function of nanotube length. As shown in the figure, the interfacial shear strength is independent of the nanotube length. The average shear strength is 30.3 ± 3.2 MPa, which matches well with the 26.3 MPa value obtained by Bichoutskaia [2005] for double-walled nanotubes using an *ab initio* method. Similarly, the interfacial shear strength between a nanotube and epoxy is about 11.2 ± 0.7 MPa, as shown in Figure 14. Since we only consider the Van der Waals force at the interface, it is reasonable that the interfacial shear strength between nanotube and epoxy is smaller than that between nanotube ropes. This is caused by two reasons: (i) the minimum distance between carbon atoms in the inner and outer nanotubes is smaller than that between a carbon atom in nanotube and the other atoms in the surrounding polymer; (ii) the hydrogen atoms in the polymer occupy much space and contribute a very small Van der Waals energy to the system, hence weakening the interfacial strength of the polymer.

The MD model serves a good starting point and can be extended in the future to examine the interfacial shear strength caused by electrostatic force and others. The calculated interfacial shear strength can be integrated with the micro-mechanics and viscoelastic models discussed in the previous sections to predict the overall materials and structure damping level.

Nanofiller alignment

Analysis results in the Penn State investigation [Liu et al., 2006a,b] have indicated that a great

improvement of loss factor could be achieved by dispersing and aligning CNTs or nanoropes in the polymeric materials when the applied stress in the alignment direction was high enough to cause complete sliding of all the nanofillers. This finding indicates that to further significantly enhance CNT-composite damping, we should explore the feasibility of CNT alignment in such composites.

Methods of orienting CNTs in polymers based on viscous fluid flow [Thostenson and Chou, 2002; Mayer et al., 2002; Xu et al., 2002; Zhang et al., 2005], and magnetic field [Kimura et al., 2002; Smith et al., 2000] have been demonstrated previously, although the investigators believe that these methods are not amenable to epoxy resins and composites. Rather, the use of electrical fields to manipulate the orientation of CNTs is seen as a more promising method for further development and application to the problem at hand [Adamson and Gast, 1997].

By applying an electric field on a suspension of particles in a liquid medium, surface charges are induced on the particles, the details of which depend on the physical and chemical properties of the particles and the medium. The acquired charge generates an electrostatic potential around the particle known as the zeta potential. The motion of the particle is controlled by the interaction between the zeta potential and the applied electric field, known as electrokinetics, and can be predicted by using models developed in [Holtzer and Velegol, 2005; Ye et al., 2002; Solomentsev and Anderson, 1994; Fair and Anderson, 1989].

A first attempt at Penn State to align vapor-grown carbon nanofibers (Pyrograph III) in epoxy using an electric field resulted in samples with anisotropic conductivities. The liquid CNF/epoxy mixture was cured while applying a uniform AC electric field of 100 V/cm at 60 Hz. Figure 15 shows a plot of AC impedance of cured samples as a function of AC frequency. The impedance of the sample cured under the influence of electric field shows no dependence on frequency in the direction of electric field applied during curing, but a frequency dependent behavior is observed in the direction transverse to the field. The frequency independent behavior of impedance parallel to the direction of the field applied during curing is an indicator of a good conducting network in the specimen. Note that cured epoxy with no nanofiller is generally nonconductive in this range of measurements. Figure 15 also provides a comparison between the AC impedances of specimens made with and without electric field. The impedance of the specimen made without electric field is highly dependent on the frequency of applied field, indicating a poor conducting network in a randomly oriented nanofiber specimen. These preliminary results verify the formation of good conducting networks of nanofibers using an electric field, but do not necessarily indicate alignment.

We next investigated the suitability of DC and AC electric fields in aligning CNFs in epoxy at elevated temperatures. The interest in elevated temperatures comes from the fact that many high performance thermoset epoxies cure at around 100°C. At these elevated temperatures, the viscosity of the epoxy reduces considerably in comparison to the room temperature viscosity, thus changing the electrokinetics of the CNFs. To investigate the translation and rotation of CNFs in epoxy under realistic curing temperatures, the movement of CNFs at elevated temperatures was observed using an optical microscope. An electrophoresis cell was constructed using a glass slide and a cover glass for measuring the electrophoretic mobility and rotational kinetics. A DC electric field with field strength of 100 V/cm and AC electric fields with various

field strengths and frequencies were applied while the mobility and rotation of the CNFs were recorded using a CCD camera attached to the microscope.

(i) *Effect of DC electric field*

Figure 16 shows pictures of CNFs in epoxide just before applying a DC electric field and after 3 and 6 seconds of continuous application of field at 90°C. The distance between the electrodes was 0.04 inch (1 mm) and the field strength was 10 VDC. Figure 16(a) shows the initial random orientation of the CNFs just after filling the cell with the mixture. On application of the electric field the nanofibers rotated as they translated towards the positive electrode. The movement of the CNFs towards the positive electrode suggests that they are negatively charged in the epoxy. The CNFs were found to “porpoise” in the plane of view as they translated. This behavior resembles the undulating motion of a swimming porpoise. It was not possible to align all the CNFs at the same time in epoxy with a DC field (Figure 16(c)). Moreover, the continuous application of DC electric field forced all the CNFs close to the positive electrode. Due to the above mentioned reasons, DC electric field is considered not suitable for alignment at elevated temperatures.

(ii) *Effect of AC electric field*

To overcome the identified limitations of DC fields in aligning CNFs, AC electric fields were evaluated at various frequencies and electric field strengths at 90°C. The distance between the electrodes was 0.04 inch (1 mm) and the field strength was 20 Vrms. Figure 17 shows the average rate of rotation for CNFs having different aspect ratios (length divided by diameter, l/d) for various frequencies and strengths of AC electric field. The electric field was applied for 10-30 seconds to let the particles rotate and align in the direction of electric field. Two general trends observed in Figure 17 are (i) the rate of rotation increases with the applied frequency and the strength of electric field, and (ii) the particles with smaller aspect ratio rotate faster than the higher aspect ratio particles.

The continuous application of AC electric field not only aligns the particles, but also forms continuous chains of CNFs by the dipole-dipole interaction (Figure 18). CNFs suspended in liquid epoxy are polarized by the electric field and therefore experience electrostatic torque due to the interaction of their charge and the applied field. Furthermore, oriented and polarized particles experience an attraction towards each other due to the dipole-dipole interaction and form a network of chains between the electrodes. The alignment and structure of the CNF chains were varied as functions of AC frequency. The alignment was investigated at a temperature of 121°C with a gap of 0.04 inch (1 mm) between the electrodes. Partial chains grew from both the electrodes and joined roughly in the center of the cell to form complete chains spanning the electrode gap. It was also observed that the morphology of the chains of aligned CNFs is dependent on the frequency of electric field. As can be seen in Figure 19, the higher tested frequencies (100 kHz & 1 MHz) resulted in denser chain patterns or, in other words, more chains per unit area of the composite. However, there exists a practical constraint in using high frequencies: i.e., the need for specialized electrical equipment to generate high enough voltages (~100 Vrms) at these frequencies to align over large distances (~cm).

(iii) *Use of high strength AC electric field in manufacturing composites*

In order to better realize the potential of aligned carbon nanofillers for enhancing the damping properties of structural composites, there is a need to align and network nanofillers over distances greater than a few millimeters. Moreover, to be able to assess the derived benefits from alignment, specimens having a length of a few centimeters are required for testing by tension or dynamic mechanical analysis, for example. Since the maximum applied voltage at 1 MHz was limited to 50 Vrms by the available equipment, it was decided to use 1 kHz for alignment, because high voltages in the range of 100s of volts can be easily generated using the voltage amplifier without excessively reducing the chain density.

The aim of these experiments is to demonstrate the ability to make cured cm-sized specimens of epoxy with chains of aligned CNFs. The test temperature was 121°C at which it took about an hour for the epoxy/amine system to cure. The distance between the electrodes was selected as 2.5 cm and the width of the cell was selected as 5 cm. A 145 Vrms electric field strength and 0.1 wt% CNF concentration were used. At 1 kHz, the chains of CNF aligned and spanned the distance between the electrodes within 6 minutes (Figure 20). After curing the composites, rectangular specimens of approximate dimensions 50×25×0.3 mm were successfully removed from the mold as shown in Figure 21.

The future efforts in realizing the objective of high damping composites would require simulation (MD) and experimental verification of the pullout process of nanotubes/ropes from surrounding polymeric material. This includes further refinement and extension of the manufacturing processes developed thus far for CNFs to include CNTs as well. Interfacial strength needs to be determined by back-calculation of quasi-static stress-strain behavior of polymer reinforced with highly aligned nano-reinforcements. This information should then be evaluated in light of the simulation results to validate the model. Based on the validated models, optimum types and orientations of fillers for achieving polymer with high damping, light weight, and low bulk can be determined.

References:

Adamson, A. W., and Gast, A. P., 1997, *Physical Chemistry of Surfaces*, John Wiley & Sons, New York.

Bichoutskaia, E, Popov, A.M., El-Barbary, A., Heggie, M.I., and Lozovik, Y.E., 2005, “*Ab initio* Study of Relative Motion of Walls in Carbon Nanotubes”, *Physical Review B* (71), pp. 113403-113406.

Cooper, C. A., Cohen, S. R., Barber, A. H., Wagner, H. D., 2002, “Detachment of Nanotubes from a Polymer Matrix,” *Applied Physics Letters*, 81(20), pp. 3873-3875.

Fair, M.C., and Anderson, J.L., 1989, “Electrophoresis of Nonuniformly Charged Ellipsoidal Particles,” *Journal of Colloid and Interface Science*, 127(2), pp. 388-400.

Frankland, S. J. V., Banderawalla, T., Gates, T. S., 2003, “Calculation of Non-Bonded Forces due to Sliding of Bundled Carbon Nanotubes,” *Proc. 44th AIAA/ASME/ASCE/AHS/ASC Structures, Structural Dynamics, and Materials Conference*, Vol. 2, AIAA, Reston, VA, pp. 1252-1262.

- Holtzer, G. L., Velegol, D., 2005, "Limitations of Differential Electrophoresis for Measuring Colloidal Forces: A Brownian Dynamics Study," *Langmuir*, 21(22), pp. 10074-10081.
- Kimura, T., Ago, H., Tobita, M., Ohshima, S., Kyotani, M., Yumura, M., 2002, "Polymer Composites of Carbon Nanotubes Aligned by a Magnetic Field," *Advanced Materials*, 14, pp. 1380-1383.
- Liu, A, Huang, J. H., Wang, K. W., Bakis, C. E., 2006 a, "Effects of Interfacial Friction on the Damping Characteristics of Composites Containing Randomly Oriented Carbon Nanotube Ropes," *Journal of Intelligent Material Systems and Structures*, 17, pp. 217-229.
- Liu, A., Wang, K. W., Bakis, C. E., Huang, J. H., 2006 b, "Analysis of Damping Characteristics of a Viscoelastic Polymer Filled with Randomly Oriented Single-Wall Nanotube Ropes," *SPIE Conf. on Smart Structures and Materials*, San Diego, CA.
- Mayer, J. J., Cooper, C. A., Ravich, D., Lips, D., Wagner, H. D., 2002, "Distribution and Alignment of Carbon Nanotubes and Nanofibrils in a Polymer Matrix," *Composites Science and Technology*, 62, pp. 1105-1112.
- Smith, B.W., Benes, Z., Luzzi, D.E., Fischer, J.E., Walters, D.A., Casavant, M.J., Schmidt, J., Smalley, R.E., 2000, "Structural Anisotropy of Magnetically Aligned Single Wall Carbon Nanotube Films," *Applied Physics Letters*, 77, pp. 663-665.
- Solomentsev, Y., Anderson, J. L., 1994, "Electrophoresis of Slender Particles," *Journal of Fluid Mechanics*, 279, pp. 197-215.
- Thostenson, E. T., and Chou, T-W., 2002, "Aligned Multi-walled Carbon Nanotube-reinforced Composites: Processing and Mechanical Characterization," *Journal of Physics D: Applied Physics*, 35, pp. L77-L80.
- Wong, M., Paramsothy, M., Xu, X. J., Ren, Y., Li, S., and Liao, K., 2003, "Physical Interaction at Carbon Nanotube- Polymer Interface," *Polymer* 44(25), pp. 7757-7764.
- Xu, X., Thwe, M. M., Shearwood, C. and Liao, K., 2002, "Mechanical Properties and Interfacial Characteristics of Carbon-nanotube-reinforced Epoxy Thin Films," *Applied Physics Letters*, 81, pp. 2833-2835.
- Ye, C., Sinton, D.; Erickson, D.; Li, D., 2002, "Electrophoretic Motion of a Circular Cylindrical Particle in a Circular Cylindrical Microchannel," *Langmuir*, 18 (23), pp. 9095-9101.
- Zhang, M., Fang, S., Zakhidov, A., Lee, S., Aliev, A., Williams, C., Atkinson, K., and Baughman, R., 2005, "Strong, Transparent, Multifunctional, Carbon Nanotube Sheets," *Science*, 309, pp. 1215-1219.

LIST OF PUBLICATIONS

Referred journal publication

- X. Zhou, E. Shin, K. W. Wang, and C. E. Bakis, "Interfacial Damping Characteristics of Carbon Nanotube-Based Composites," *Composites Science and Technology*, 64(15), pp. 2425-2437, 2004.

A. Liu, J. H. Huang, K. W. Wang, C. E. Bakis, “Effects of Interfacial Friction on the Damping Characteristics of Composites Containing Randomly Oriented Carbon Nanotube Ropes,” *Journal of Intelligent Material Systems and Structures*, 17, pp. 217-229, 2006.

Conference publications and presentations

Ailin Liu, K. W. Wang, Charles E. Bakis, Jin H. Huang, “Analysis of Damping Characteristics of a Viscoelastic Polymer Filled with Randomly Oriented Single-Wall Nanotube Ropes,” *SPIE Conf. on Smart Structures and Materials*, San Diego, CA, 2006.

PARTICIPANTS AND DEGREES AWARDED

Personnel supported: K. W. Wang (PI), Charles Bakis (Co-PI), Xu Zhou (Post doc fellow), Jin H. Huang (Visiting scholar), Ailin Liu (Ph.D. student), Ambuj Sharma (Ph.D. student).

Table 1. Material properties used in the model for composite with randomly oriented nanoropes

Unit cell	Length	1.0 μm
	Width	1.0 μm
	Thickness	5.30 nm
Resin	Young's modulus	3.3 GPa
	Poisson's ratio	0.35
(10,10) SWNT	Young's modulus of graphite sheet	1.03 TPa *
	Shear modulus of graphite sheet	0.44 TPa *
	Radius	0.67 nm
	Length	1 μm
	Volume fraction of nanorope	0.2%
Sheath	Inner radius	2 nm
	Outer radius	2.50 nm

* Graphite sheet properties from Odegard et al, 2001

Table 2. Values of critical shear stresses used in the model for composite with randomly oriented nanoropes

	Inter-tube critical shear stress	SWNT/sheath critical shear stress
Case 1	0.5 MPa	50 MPa
Case 2	5 MPa	50 MPa
Case 3	0.5 MPa	100 MPa

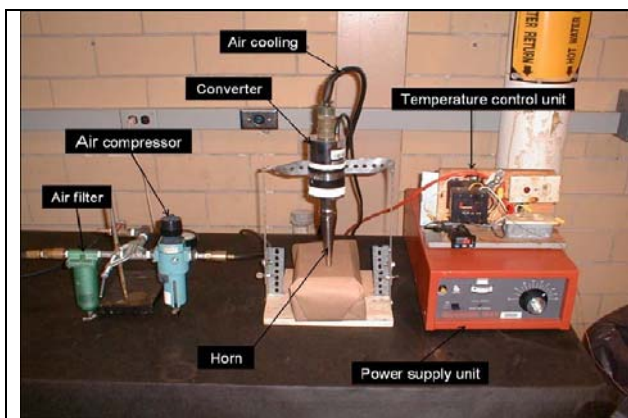


Figure 1. Ultrasonic mixer set-up used for dispersing nanotubes in resin mixture.

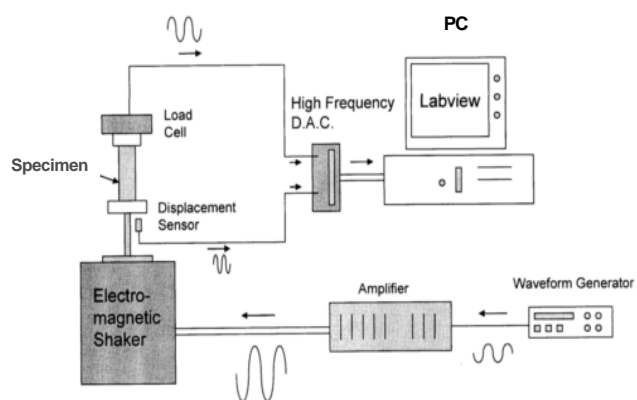


Figure 2. Loss factor measurements through dynamic testing.

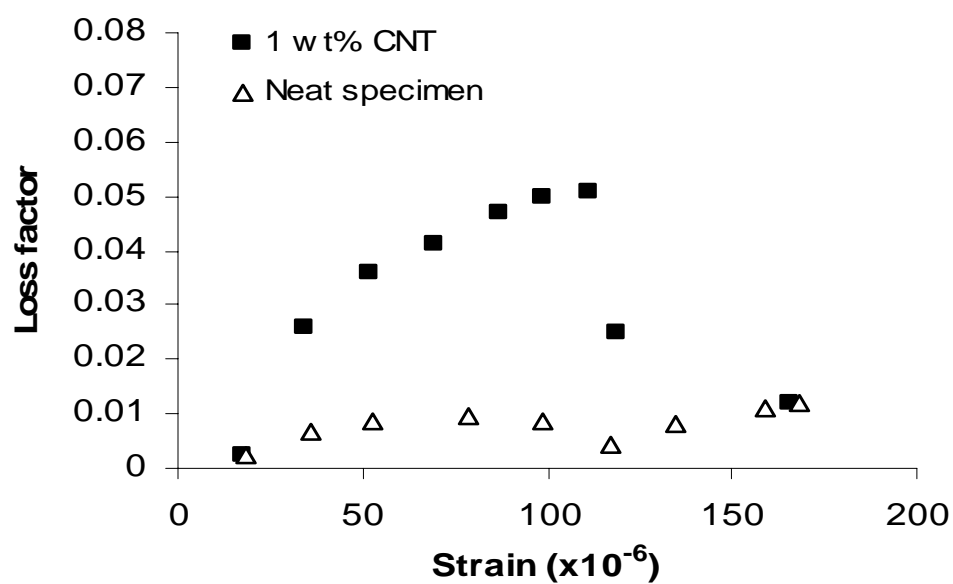
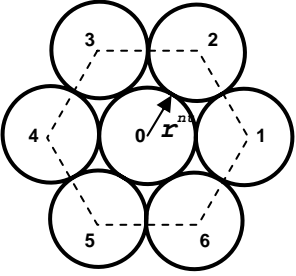
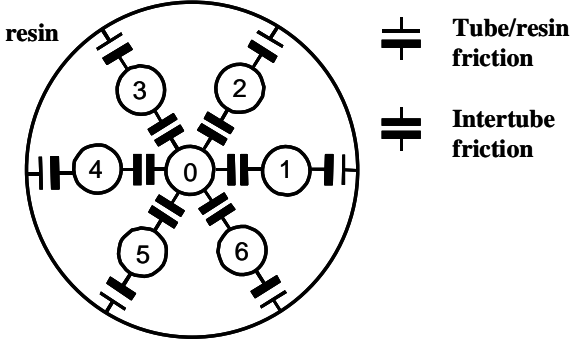


Figure 3. Loss factor vs. peak cyclic strain: neat resin and 1 wt% CNT specimens.

	
<p>Figure 4. A schematic of a nanotube lattice in hexagonal arrangement.</p>	<p>Figure 5. A schematic of load transfer in the tube lattice model.</p>

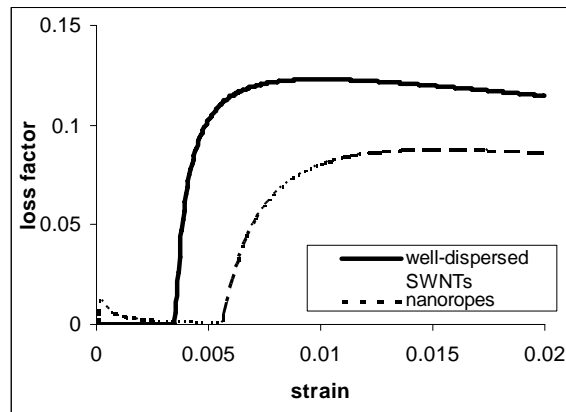


Figure 6. Loss factors: nanoropes vs nanotubes. (Unidirectionally aligned configuration)

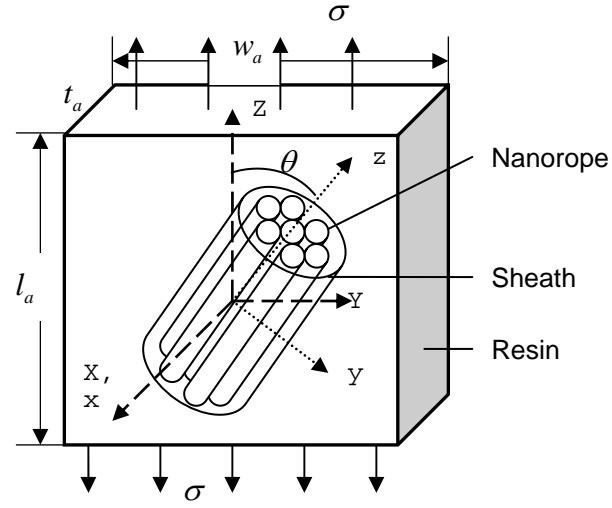


Figure 7: Unit cell consisting of a bundle of seven SWNTs (nanorope) surrounded by a sheath and remote resin.

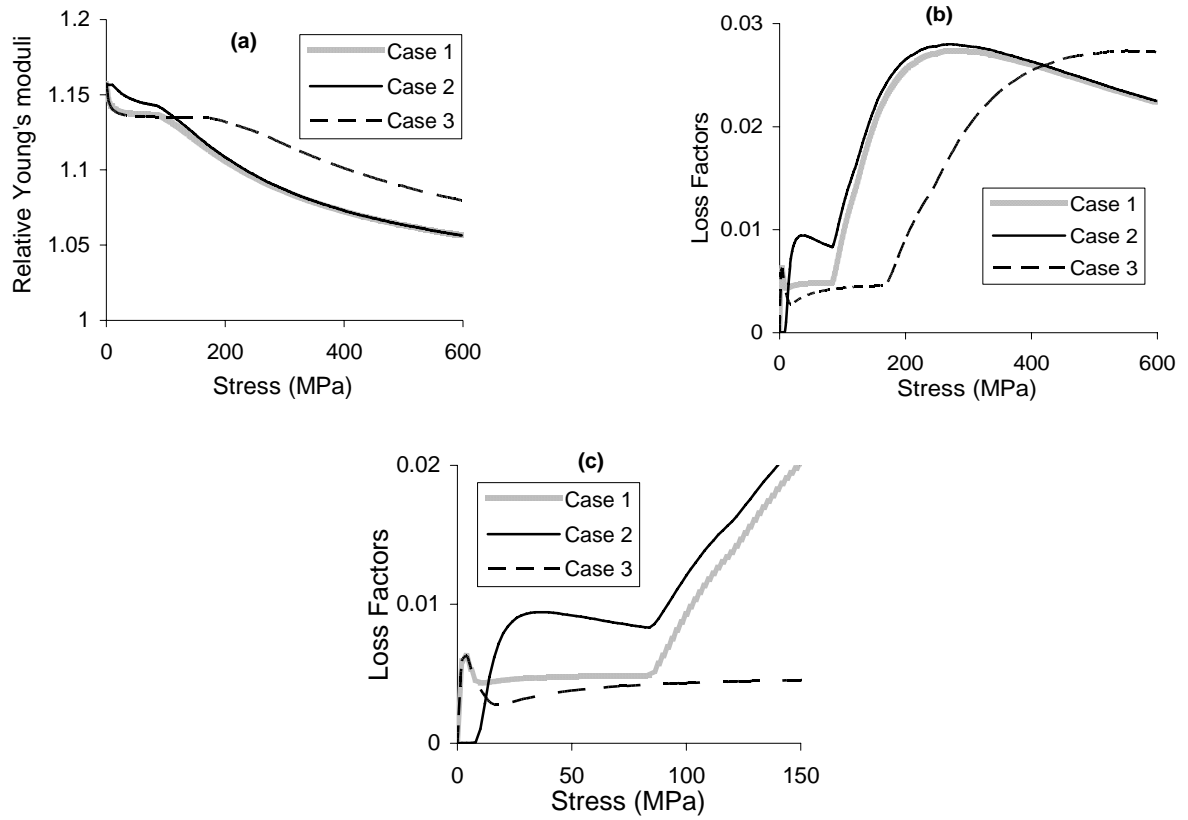


Figure 8: Comparison of composites containing randomly dispersed and oriented nanoropes: (a): Relative Young's moduli; (b): loss factors; (c) loss factors in small stress region.

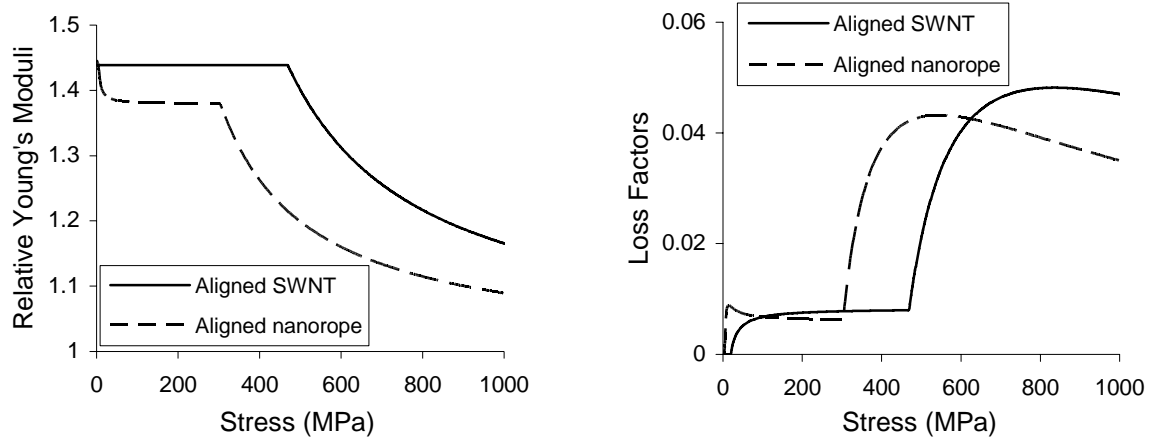


Figure 9: Comparison for composites containing aligned SWNTs and aligned nanoropes: (Left): Young's modulus relative to the resin; (Right): loss factors

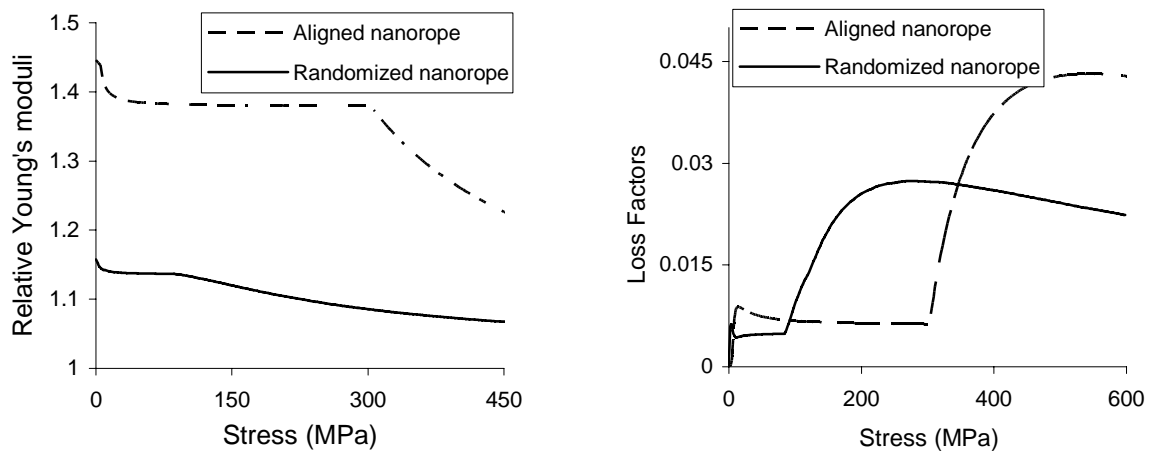


Figure 10: Comparison for composites containing aligned nanoropes and randomly dispersed nanoropes: (Left): Young's modulus relative to the resin; (Right): loss factors

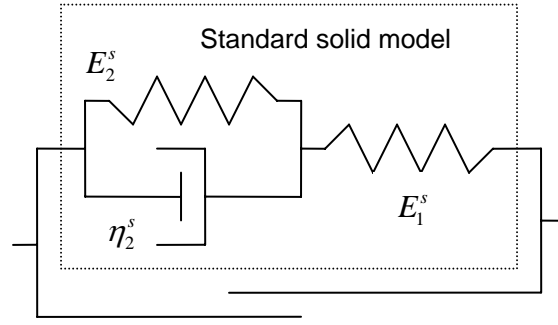


Figure 11. Composites using standard solid model($E_1^s = 3.3GPa$, $E_2^s = 3.3GPa$, $\eta_2^s = 50GPa \cdot s$)

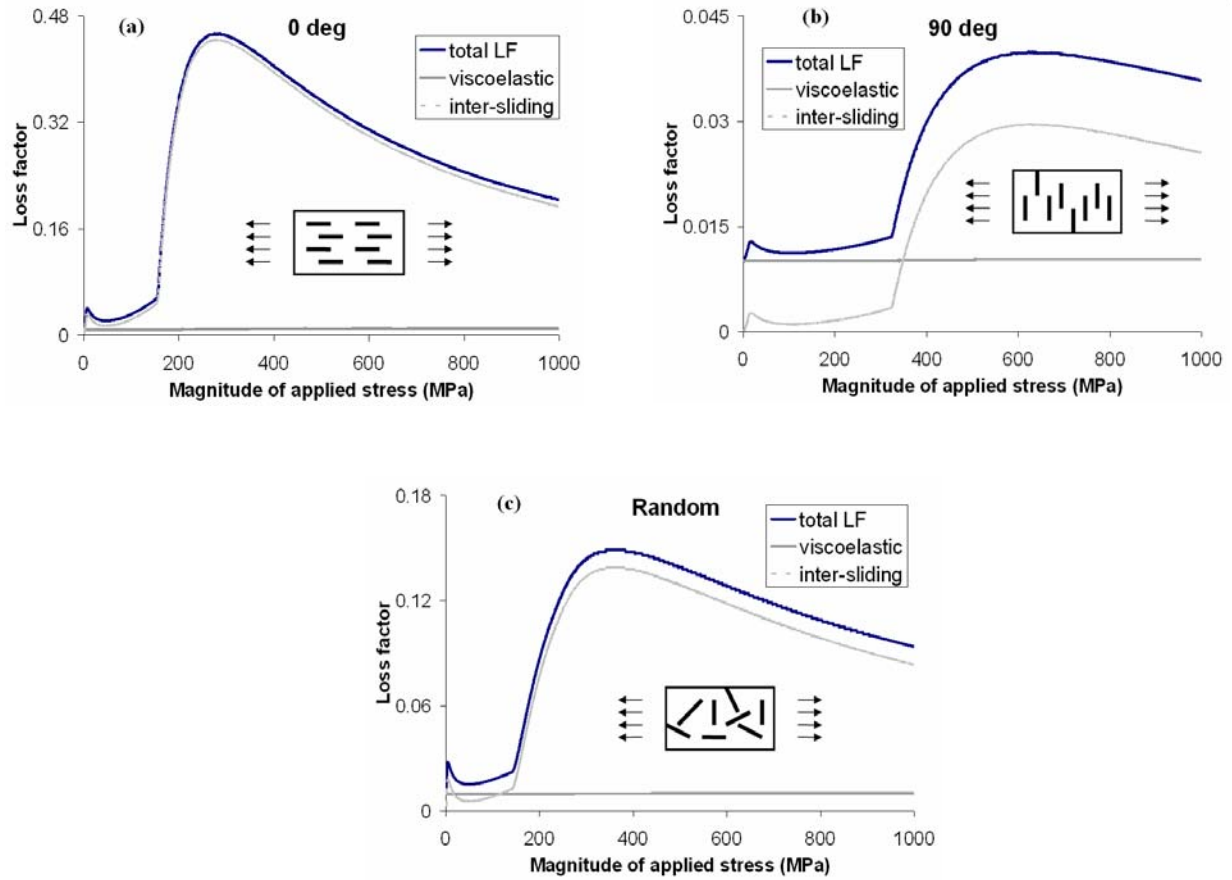


Figure 12. Loss factors vs. magnitude of applied stress: (a) composite with aligned nanoropes and load along nanorope direction; (b) composite with aligned nanoropes and load in the direction perpendicular to nanorope direction; (c) composite with randomly oriented nanoropes

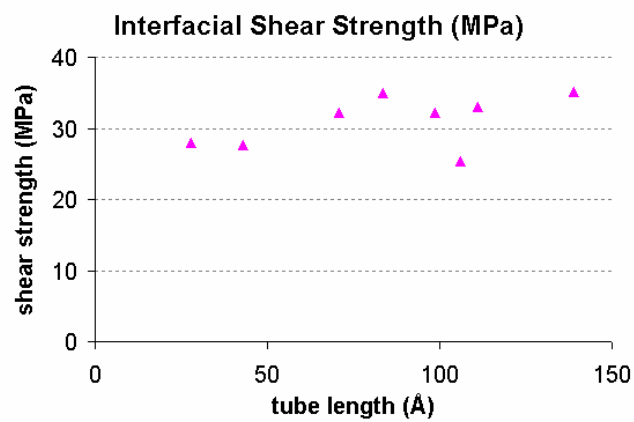


Figure 13. Interfacial shear strength between nanotube ropes as a function of tube length

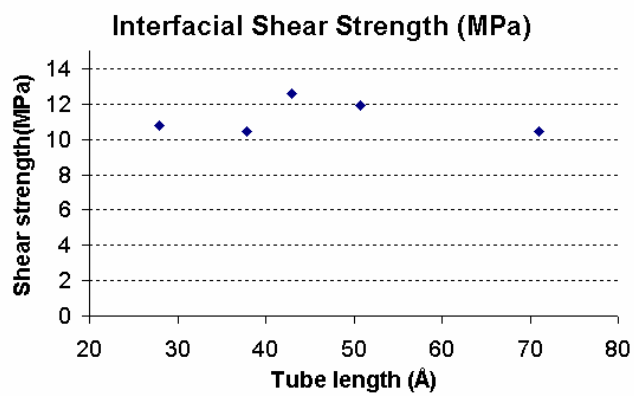


Figure 14. Interfacial shear strength between nanotube and epoxy as a function of tube length

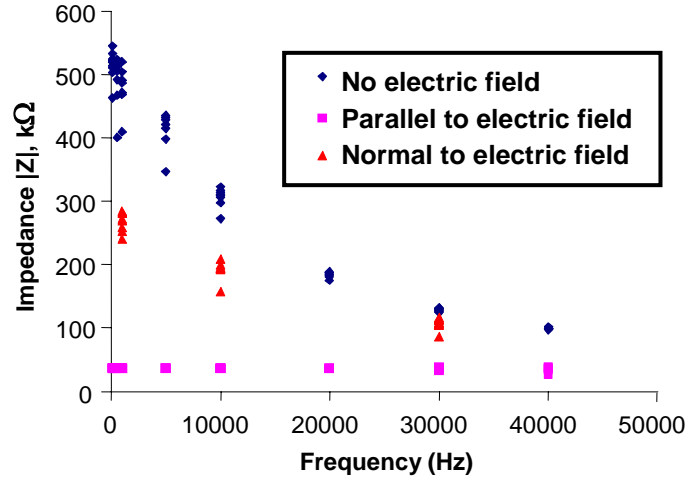


Figure 15 Electrical measurements on aligned and random nanofiber composites

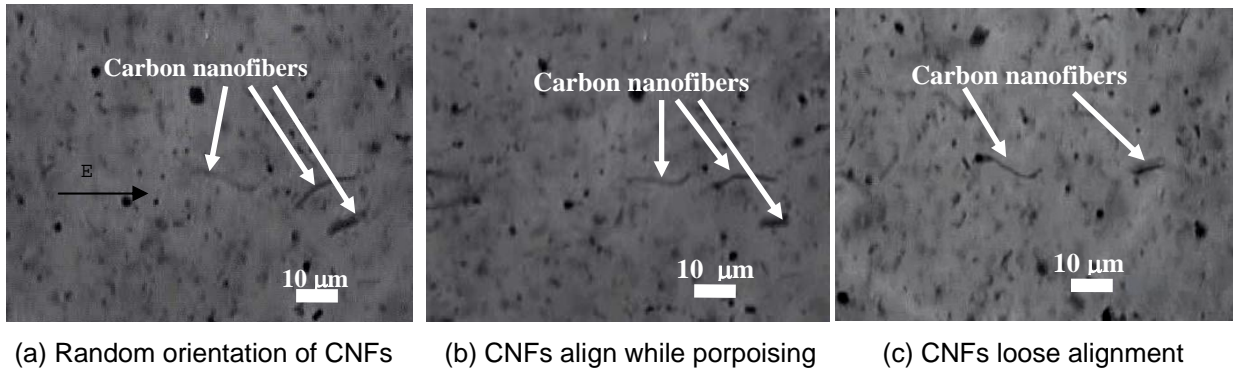


Figure 16. Effect of DC electric field on the alignment of CNFs in epoxy

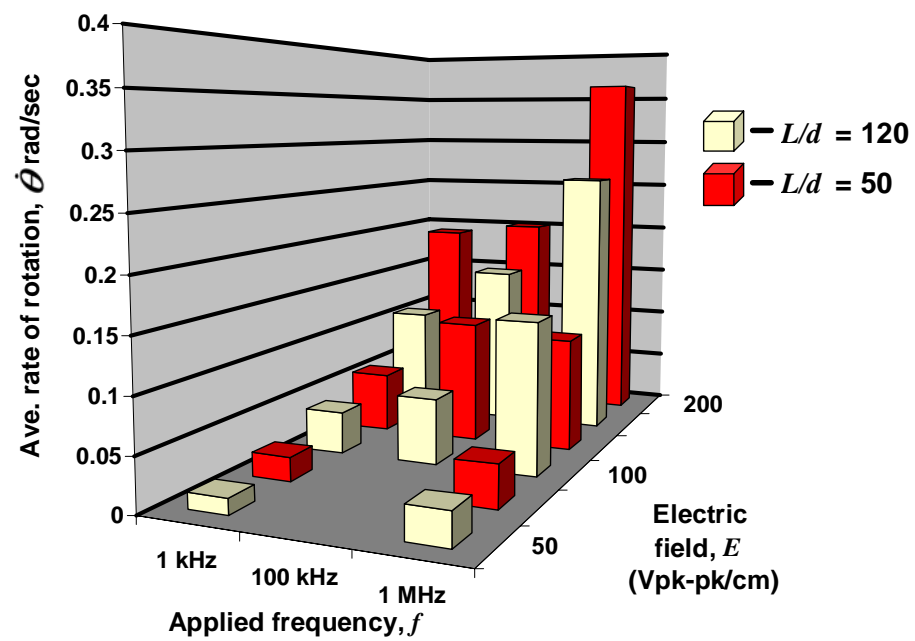


Figure 17. Kinetics of CNF alignment in AC electric field

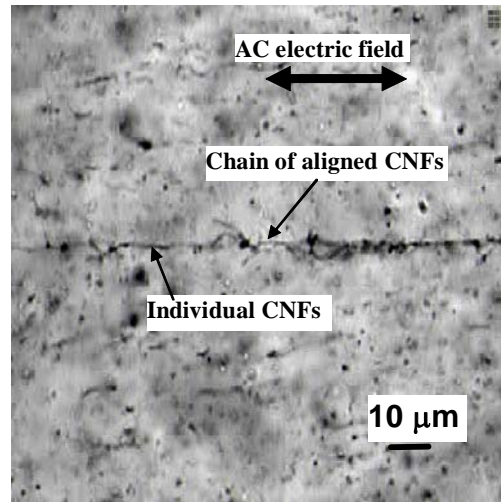


Figure 18. Chain of aligned CNFs in the direction of AC electric field

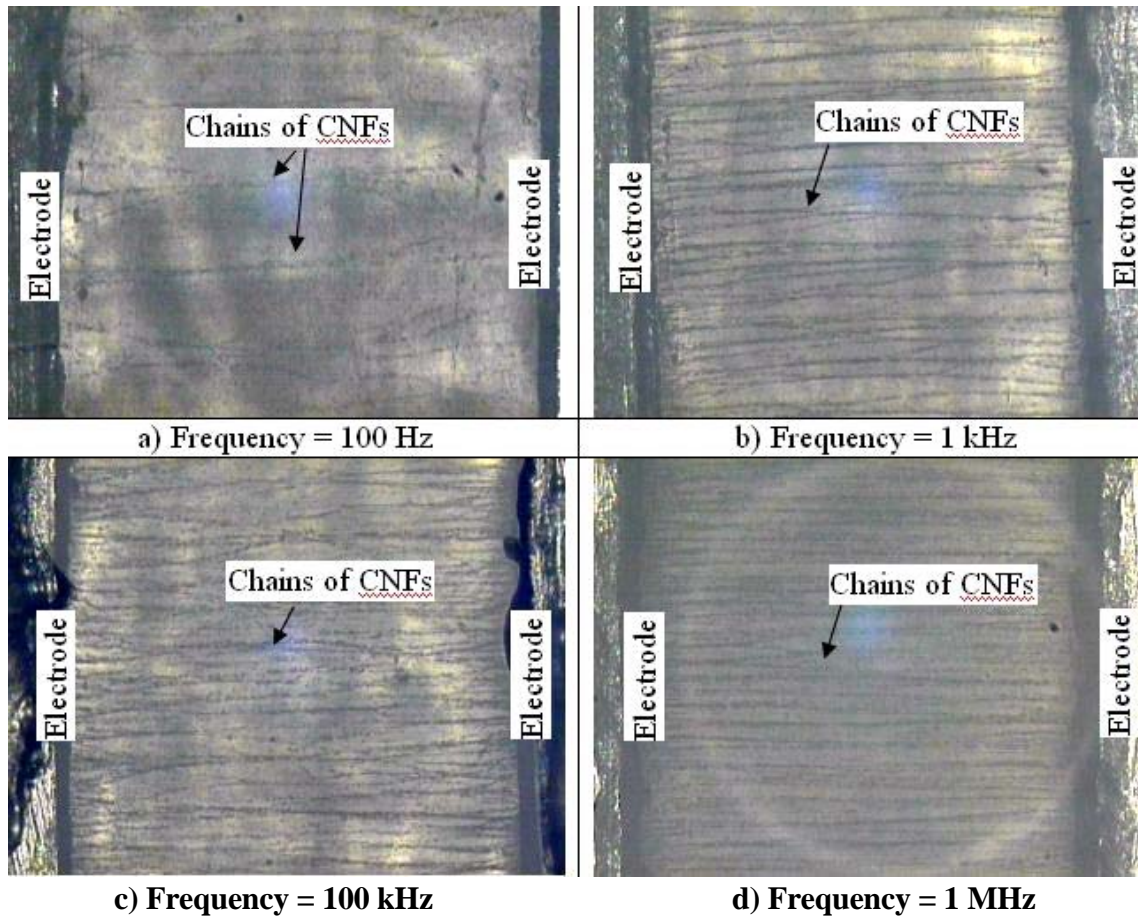


Figure 19. Chains of CNFs in epoxy bridging the gap between the electrodes at various AC frequencies ($V_{\text{rms}} = 50 \text{ V}$; distance between electrodes = 1 mm)

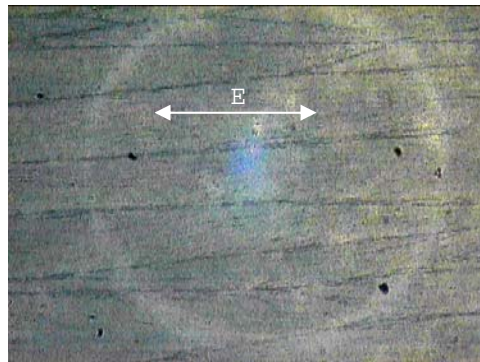


Figure 20. Chains of 0.1 wt% aligned CNFs in a fully cured epoxy

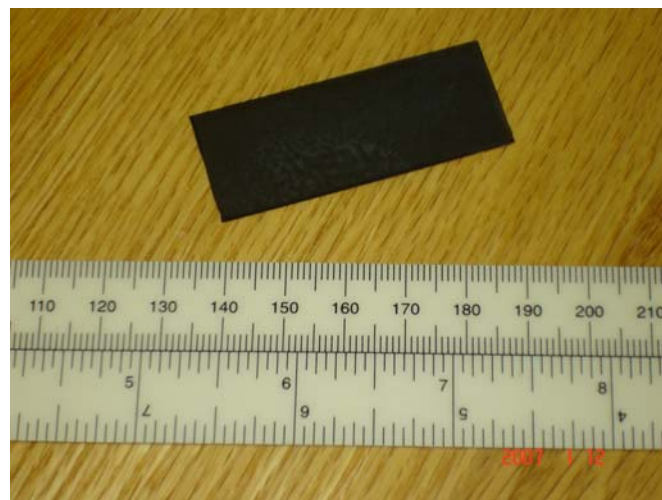


Figure 21. Fully cured 0.1 wt% aligned CNF/epoxy composite